Specific viscosity of neutron-rich nuclear matter from the relaxation time approach

Jun Xu[1, *]

[1]*Cyclotron Institute, Texas A&M University, College Station, Texas 77843-3366, USA*
(Dated: December 6, 2011)

The specific viscosity of neutron-rich nuclear matter is studied from the relaxation time approach using an isospin- and momentum-dependent interaction and the nucleon-nucleon cross sections taken as those from the experimental data modified by the in-medium effective masses as used in the IBUU transport model calculations. The relaxation time of neutrons is larger while that of protons is smaller in neutron-rich nuclear matter compared with that in symmetric nuclear matter, and this leads to a larger specific viscosity in neutron-rich nuclear matter. In addition, the specific viscosity decreases with increasing temperature because of more frequent collisions and weaker Pauli blocking effect at higher temperatures. At lower temperatures the specific viscosity increases with increasing density due to the Pauli blocking effect, while at higher temperatures it slightly decreases with increasing density as a result of smaller in-medium effective masses at higher densities.

I. INTRODUCTION

The properties of nuclear matter under extreme conditions is one of the major problems in nuclear physics. Transport models are now widely used in studying the equation of states (EOS) of the nuclear matter formed in intermediate-energy heavy-ion collisions [1]. It was found that the transverse flow from the experimental data can be reproduced by the transport model calculation using a stiff EOS together with a momentum-independent potential or a soft EOS together with a momentum-dependent potential [2]. However, the extracted incompressibility from Giant Monopole Resonance experiments is 231 ± 5 MeV [3], indicating a soft EOS and the importance of the momentum-dependent mean field potential. Recently, an isospin- and momentum-dependent interaction together with the Isospin-dependent Boltzmann-Uehling-Uhlenbeck (IBUU) transport model has been extensively used to study the dynamics in intermediate-energy heavy-ion collisions. Especially, extensive studies have been done to extract the information on the isospin-dependent part of the EOS, i.e., symmetry energy, from isospin diffusion [4], neutron/proton [5] and triton/^{3}He [6] ratios and differential flows, and π^-/π^+ ratio [7]. For a recent review, I refer the readers to Ref. [8].

Although hydrodynamic models have seldom been used in intermediate-energy heavy-ion collisions [9], they are widely used in relativistic heavy-ion collisions, where a very strong interacting matter called quark-gluon plasma (QGP) is formed. It has been found that this matter has a very small viscosity and behaves like a nearly perfect fluid. Below the temperature $T_c = 170 \sim 180$ MeV hadronization happens and the viscosity of the system increases. Although there have already been extensive studies on the shear viscosity of the QGP [10–13] and that of the relativistic hadron gas [14–17], only a

few studies have been devoted to the viscosity of nuclear matter formed in intermediate-energy heavy-ion collisions [18–22]. Even fewer studies have been devoted to the isospin dependence of the viscosity [23]. It is thus of great interesting to study the viscosity of the neutron-rich nuclear matter, especially its isospin dependence, formed in the intermediate-energy heavy-ion collisions as in the IBUU transport model.

Many methods in the literature have been used to study the viscosity [12, 15, 18, 24], among which directly using Green-Kubo formulas is the first-principle way of the study [25]. In the present study the relaxation time approach is used [26, 27]. This approach is helpful in studying how the Pauli blocking, in-medium cross sections and in-medium effective masses will affect the shear viscosity and can give qualitative ideas how the shear viscosity changes with density, temperature and isospin asymmetry of the nuclear matter.

This paper is organized as follows. The isospin- and momentum-dependent interaction (here after 'MDI') is briefly reviewed in Sec. II. The method to calculate the shear viscosity from the relaxation time approach is given in Sec. III. In Sec. IV the results of the relaxation time and the specific viscosity are shown and the effects from isospin, temperature and Pauli blocking are discussed. A summary is given in Sec.V.

II. THE ISOSPIN- AND MOMENTUM-DEPENDENT INTERACTION

The MDI interaction is a modified finite-range Gogny-like interaction [28], and it was recently found that the effective nucleon-nucleon potential is composed of a zero-range many-body term and a finite-range Yukawa term [29]. In the mean-field approximation, the single-particle potential for a nucleon with momentum $\vec{p}$ and

*Electronic address: xujun@comp.tamu.edu

isospin τ in a nuclear matter medium is written as

$$
\begin{aligned}
U_\tau(\vec{p}) &= A_u(x)\frac{\rho_{-\tau}}{\rho_0} + A_l(x)\frac{\rho_\tau}{\rho_0} \\
&+ B(\frac{\rho}{\rho_0})^\sigma(1 - x\delta^2) - 8\tau x\frac{B}{\sigma+1}\frac{\rho^{\sigma-1}}{\rho_0^\sigma}\delta\rho_{-\tau} \\
&+ \frac{2C_{\tau,\tau}}{\rho_0}\int\frac{d^3p'}{(2\pi)^3}\frac{f_\tau(\vec{p'})}{1+(\vec{p}-\vec{p'})^2/\Lambda^2} \\
&+ \frac{2C_{\tau,-\tau}}{\rho_0}\int\frac{d^3p'}{(2\pi)^3}\frac{f_{-\tau}(\vec{p'})}{1+(\vec{p}-\vec{p'})^2/\Lambda^2}.
\end{aligned} \tag{1}
$$

In the above $\tau = 1/2$ ($-1/2$) for neutrons (protons); $\delta = (\rho_n - \rho_p)/\rho$ is the isospin asymmetry with $\rho_n(\rho_p)$ being the neutron (proton) density and $\rho = \rho_n + \rho_p$ being the total density of the medium; $f_\tau(\vec{p})$ is the local phase space distribution function and it can be written as

$$
f_\tau(\vec{p}) = dn_\tau(\vec{p}) = \frac{d}{\exp\left[(\frac{p^2}{2m} + U_\tau(\vec{p}) - \mu_\tau)/T\right] + 1}, \tag{2}
$$

where $d = 2$ is the spin degeneracy and $n_\tau(\vec{p})$ is the occupation probability. m is the nucleon mass, T is the temperature and μ_τ is the proton or neutron chemical potential and can be determined from

$$
\rho_\tau = \int f_\tau(\vec{p})\frac{d^3p}{(2\pi)^3}. \tag{3}
$$

From a self-consistent iteration method [30], both the single-particle potential and the distribution function can be calculated numerically. The entropy density of the nuclear matter can thus be calculated from

$$
s = -\sum_\tau d\int[n_\tau\ln n_\tau + (1-n_\tau)\ln(1-n_\tau)]\frac{d^3p}{(2\pi)^3} \tag{4}
$$

The detailed values of the parameters $A_u(x)$, $A_l(x)$, σ, B, $C_{\tau,\tau}$, $C_{\tau,-\tau}$ and Λ can be found in Ref. [28] and they are assumed to be independent of the temperature. These parameters lead to the binding energy $E_0 = -16$ MeV, the incompressibility $K_0 = 211$ and the symmetry energy $E_{sym} \approx 31$ MeV at the saturation density $\rho_0 = 0.16$ fm^{-3}. The parameter x is used to mimic the density dependence of the symmetry energy while keeping the properties of symmetric nuclear matter unchanged. Comparison between the results from the IBUU transport model calculation with the experimental results of isospin diffusion data leads to $-1 < x < 0$ at subsaturation densities [4, 31] and with that of π^-/π^+ ratio somehow leads to a super soft symmetry energy $x = 1$ at suprasaturation densities [7]. In the following $x = 0$ is used if not addressed.

Once the momentum dependence of the single-particle potential is obtained, the effective mass of a nucleon with isospin τ in the nuclear matter medium can be calculated from

$$
\frac{1}{m_\tau^\star} = \frac{1}{m} + \frac{1}{p}\frac{dU_\tau}{dp}. \tag{5}
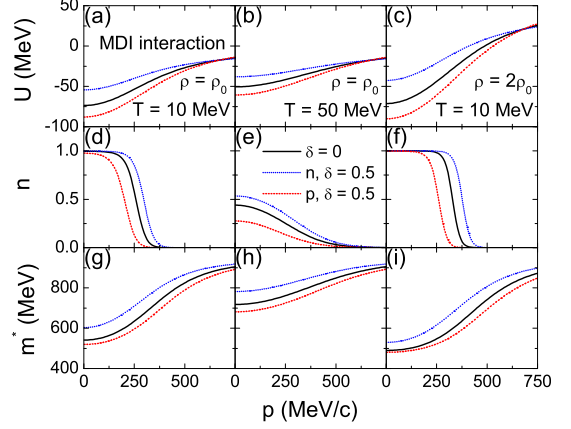$$

FIG. 1: (color online) Momentum dependence of the single-particle potential, the occupation probability and the effective mass at $\rho = \rho_0$ and $T = 10$ MeV ((a), (d), (g)), $\rho = \rho_0$ and $T = 50$ MeV ((b), (e), (h)), and $\rho = 2\rho_0$ and $T = 10$ MeV ((c), (f), (i)) from the MDI interaction. Results from symmetric ($\delta = 0$) nuclear matter and neutron-rich ($\delta = 0.5$) nuclear matter are compared.

In Fig. 1 the momentum dependence of the single-particle potential, the occupation probability and the effective mass are displayed at different densities and temperatures. It is seen that the momentum-dependence of the single-particle potential is weaker at higher temperatures, which leads to a larger effective mass with increasing temperature. A higher temperature also leads to a more diffusive Fermi surface. At higher densities, the effective mass is smaller and the distribution function becomes less diffusive. The effective mass of neutrons is larger than that of protons in neutron-rich nuclear matter from the MDI interaction. This leads to a symmetry potential $U_{sym} = (U_n - U_p)/\delta$ that is consistent with the energy dependence of the Lane potential constrained by the nucleon-nucleus scattering experimental data as discussed in Ref. [32]. The relation between the shear viscosity and these single-particle properties will be discussed in the following.

III. SHEAR VISCOSITY FROM THE RELAXATION TIME APPROACH

In the present work I study the shear viscosity of an isospin asymmetric nuclear matter with uniform and static neutron and proton density ρ_n and ρ_p, respectively, and temperature T. The static flow field in the nuclear system is assumed to be in the z direction and the magnitude changes linearly with x, i.e., $u_z = cx$, $u_x = u_y = 0$. The equilibrium momentum distribution n^0 is a Fermi-Dirac distribution as Eq. (2) in the local frame while it is shifted by $m\vec{u}$ with the flow field in the lab frame. Due to collisions, the momentum distribution may differ

slightly from the equilibrium one and is written as n and $\delta n = n - n^0$ is their difference.

The shear force between flow layers per unit area is [26]

$$F = \sum_\tau < (p_z - mu_z)\rho_\tau \frac{p_x}{m_\tau^\star} >$$

$$= \sum_\tau d \int (p_z - mu_z)\frac{p_x}{m_\tau^\star} n_\tau \frac{d^3p}{(2\pi)^3}. \qquad (6)$$

In the above $\rho_\tau \frac{p_x}{m_\tau^\star}$ is the flux, i.e., the number of nucleons

of isospin τ moving in the x direction per unit time per unit area, where $\frac{p_x}{m_\tau^\star}$ can be written as $\left[\frac{p_x}{m} + (\nabla_p U_\tau)_x\right]$ from Eq. (5), and $p_z - mu_z$ is the momentum transported per nucleon. It is easily seen that the contribution of n_τ^0 to the shear force is zero as the integrand is odd in p_x. Thus, the shear force can be written as

$$F = \sum_\tau \frac{d}{(2\pi)^3} \int (p_z - mu_z)\frac{p_x}{m_\tau^\star}\delta n_\tau dp_x dp_y dp_z. \qquad (7)$$

To calculate δn_τ, we start from the BUU equation using the relaxation time approximation. The isospin-dependent BUU equation is written as

$$\frac{\partial n_\tau(p_1)}{\partial t} + \vec{v} \cdot \nabla_r n_\tau(p_1) - \nabla_r U_\tau \cdot \nabla_p n_\tau(p_1) = -(d - \frac{1}{2})\int \frac{d^3p_2}{(2\pi)^3}\frac{d^3p_1'}{(2\pi)^3}\frac{d^3p_2'}{(2\pi)^3}|T_{\tau,\tau}|^2$$

$$\times \; [n_\tau(p_1)n_\tau(p_2)(1 - n_\tau(p_1'))(1 - n_\tau(p_2')) - n_\tau(p_1')n_\tau(p_2')(1 - n_\tau(p_1))(1 - n_\tau(p_2))]$$

$$\times \; (2\pi)^3\delta^{(3)}(\vec{p_1} + \vec{p_2} - \vec{p_1'} - \vec{p_2'}) - d\int \frac{d^3p_2}{(2\pi)^3}\frac{d^3p_1'}{(2\pi)^3}\frac{d^3p_2'}{(2\pi)^3}|T_{\tau,-\tau}|^2$$

$$\times \; [n_\tau(p_1)n_{-\tau}(p_2)(1 - n_\tau(p_1'))(1 - n_{-\tau}(p_2')) - n_\tau(p_1')n_{-\tau}(p_2')(1 - n_\tau(p_1))(1 - n_{-\tau}(p_2))]$$

$$\times \; (2\pi)^3\delta^{(3)}(\vec{p_1} + \vec{p_2} - \vec{p_1'} - \vec{p_2'}), \qquad (8)$$

where the terms $1 - n$ are from the Pauli blocking effect and the degeneracy $d - \frac{1}{2}$ takes identical nucleon collisions into account. In the first-order approximation, the contribution of δn_τ on the left side can be neglected and n_τ is replaced by n_τ^0. The first term on the left side vanishes as n_τ^0 is the equilibrium distribution and the system is static. By using the relation

$$\nabla_r n_\tau^0 = \frac{\partial n_\tau^0}{\partial x}\hat{x}$$

$$= \frac{n_\tau^0(p_x, p_y, p_z - mc\delta x) - n_\tau^0(p_x, p_y, p_z)}{\delta x}\hat{x}$$

$$= -mc\frac{p_z}{p}\frac{dn_\tau^0}{dp}\hat{x}, \qquad (9)$$

the second term can be calculated as

$$\vec{v} \cdot \nabla_r n_\tau^0 = \left(\frac{p_x}{m} + \frac{dU_\tau^0}{dp}\frac{p_x}{p}\right)\left(-mc\frac{p_z}{p}\frac{dn_\tau^0}{dp}\right), \qquad (10)$$

where U_τ^0 is the single-particle potential corresponding to the equilibrium distribution n_τ^0. The third term on the left side can be similarly expressed as

$$-\nabla_r U_\tau^0 \cdot \nabla_p n_\tau^0 = -\left(-mc\frac{p_z}{p}\frac{dU_\tau^0}{dp}\right)\left(\frac{p_x}{p}\frac{dn_\tau^0}{dp}\right). \qquad (11)$$

So, the left side can be expressed as

$$\frac{\partial n_\tau(p_1)}{\partial t} + \vec{v} \cdot \nabla_r n_\tau(p_1) - \nabla_r U_\tau \cdot \nabla_p n_\tau(p_1)$$

$$= \left(-\frac{\partial u_z}{\partial x}\frac{p_z p_x}{p}\frac{dn_\tau^0}{dp}\right)_{p=p_1}, \qquad (12)$$

as $c = \partial u_z/\partial x$.

The right side vanishes if $n_\tau = n_\tau^0$ when the detailed balance is satisfied. In the relaxation time approximation only $\delta n_\tau(p_1)$ is kept and the right side can be written as [26]

$$-\frac{\delta n_\tau(p_1)}{\tau_\tau(p_1)} = -(d - \frac{1}{2})\int \frac{d^3p_2}{(2\pi)^3}\frac{d^3p_1'}{(2\pi)^3}\frac{d^3p_2'}{(2\pi)^3}|T_{\tau,\tau}|^2$$

$$\times \; [\delta n_\tau(p_1)n_\tau^0(p_2)(1 - n_\tau^0(p_1'))(1 - n_\tau^0(p_2')) + n_\tau^0(p_1')n_\tau^0(p_2')\delta n_\tau(p_1)(1 - n_\tau^0(p_2))]$$

$$\times \; (2\pi)^3\delta^{(3)}(\vec{p_1} + \vec{p_2} - \vec{p_1'} - \vec{p_2'}) - d\int \frac{d^3p_2}{(2\pi)^3}\frac{d^3p_1'}{(2\pi)^3}\frac{d^3p_2'}{(2\pi)^3}|T_{\tau,-\tau}|^2$$

$$\times \; [\delta n_\tau(p_1)n_{-\tau}^0(p_2)(1 - n_\tau^0(p_1'))(1 - n_{-\tau}^0(p_2')) + n_\tau^0(p_1')n_{-\tau}^0(p_2')\delta n_\tau(p_1)(1 - n_{-\tau}^0(p_2))]$$

$$\times \; (2\pi)^3\delta^{(3)}(\vec{p_1} + \vec{p_2} - \vec{p_1'} - \vec{p_2'}), \qquad (13)$$

where $\tau_\tau(p_1)$ is the relaxation time, i.e., the average collision time for a nucleon with isospin τ and momentum p_1, which can be expressed as

$$\frac{1}{\tau_\tau(p_1)} = \frac{1}{\tau_\tau^{same}(p_1)} + \frac{1}{\tau_\tau^{diff}(p_1)}, \tag{14}$$

with $\tau_\tau^{same(diff)}(p_1)$ being the average collision time for a nucleon with isospin τ and momentum p_1 when colliding with other nucleons of same (different) isospin, and they can thus be calculated from

$$\frac{1}{\tau_\tau^{same}(p_1)} = (d - \frac{1}{2})\frac{(2\pi)^2}{(2\pi)^3} \int p_2^2 dp_2 d\cos\theta_{12} d\cos\theta \frac{d\sigma_{\tau,\tau}}{d\Omega} \left| \frac{\vec{p}_1}{m_\tau^\star(p_1)} - \frac{\vec{p}_2}{m_\tau^\star(p_2)} \right|$$
$$\times \left[n_\tau^0(p_2) - n_\tau^0(p_2)n_\tau^0(p_1') - n_\tau^0(p_2)n_\tau^0(p_2') + n_\tau^0(p_1')n_\tau^0(p_2') \right], \tag{15}$$

$$\frac{1}{\tau_\tau^{diff}(p_1)} = d\frac{(2\pi)^2}{(2\pi)^3} \int p_2^2 dp_2 d\cos\theta_{12} d\cos\theta \frac{d\sigma_{\tau,-\tau}}{d\Omega} \left| \frac{\vec{p}_1}{m_\tau^\star(p_1)} - \frac{\vec{p}_2}{m_{-\tau}^\star(p_2)} \right|$$
$$\times \left[n_{-\tau}^0(p_2) - n_{-\tau}^0(p_2)n_\tau^0(p_1') - n_{-\tau}^0(p_2)n_{-\tau}^0(p_2') + n_\tau^0(p_1')n_{-\tau}^0(p_2') \right], \tag{16}$$

where θ_{12} is the angel between $\vec{p}_1$ and $\vec{p}_2$, and θ is the angel between the total momentum $\vec{p}_{tot} = \vec{p}_1 + \vec{p}_2 = \vec{p}_1' + \vec{p}_2'$ and the relative momentum of the final state $\vec{p}_{rel} = \vec{p}_1' - \vec{p}_2'$. As for elastic collisions $|\vec{p}_1' - \vec{p}_2'| = |\vec{p}_1 - \vec{p}_2|$, their magnitude can be calculated from

$$|\vec{p}_{tot}| = \sqrt{p_1^2 + p_2^2 + 2p_1 p_2 \cos\theta_{12}}, \tag{17}$$

$$|\vec{p}_{rel}| = \sqrt{p_1^2 + p_2^2 - 2p_1 p_2 \cos\theta_{12}}. \tag{18}$$

The magnitude of $\vec{p}_1'$ and $\vec{p}_2'$ can then be obtained from

$$|\vec{p}_1'| = \frac{1}{2}\sqrt{p_{tot}^2 + p_{rel}^2 + 2p_{tot}p_{rel}\cos\theta}, \tag{19}$$

$$|\vec{p}_2'| = \frac{1}{2}\sqrt{p_{tot}^2 + p_{rel}^2 - 2p_{tot}p_{rel}\cos\theta}. \tag{20}$$

We choose the isotropic nucleon-nucleon cross sections, and in free space they are taken as the parameterized forms [33]

$$\sigma_{pp(nn)} = 13.73 - 15.04/v + 8.76/v^2 + 68.67v^4, \tag{21}$$

$$\sigma_{np} = -70.67 - 18.18/v + 25.26/v^2 + 113.85v, \tag{22}$$

where the cross sections are in mb and v is the velocity of the projectile nucleon with respect to the fixed target nucleon. The above cross sections are the same as used in the IBUU transport model calculations. Figure 2 shows the pp and np cross sections as functions of the center-of-mass energy of the two colliding nucleons from the above parameterized form. This parametrization describes very well the experimental data for the beam energy from 10 MeV to 1 GeV [33], corresponding to the center-of-mass energy $\sqrt{s}$ from 1883 MeV to 2325 MeV. It is seen that for the most probable energies the cross section is smaller for pp collisions than for np collisions.

As used in the IBUU transport model, by assuming all the matrix elements of the nucleon-nucleon interaction are the same in free space and in the medium [34], the in-medium nucleon-nucleon cross sections are modified by
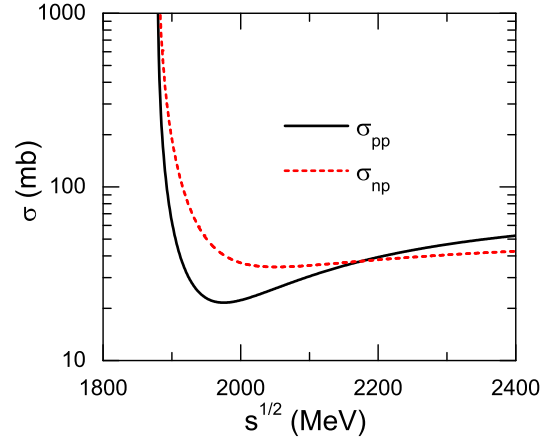

FIG. 2: (color online) pp and np cross sections in free space as functions of the center-of-mass energy of the two colliding nucleons from the parameterized form (Eqs. (21) and (22)).

the in-medium effective masses in the following form [31]

$$\sigma_{NN}^{medium} = \sigma_{NN} \left(\frac{\mu_{NN}^\star}{\mu_{NN}}\right)^2, \tag{23}$$

where μ_{NN} ($\mu_{NN}^\star$) is the free-space (in-medium) reduced mass of colliding nucleons.

Eqs. (12) and (13) lead to

$$\delta n_\tau(p) = \tau_\tau(p)\frac{\partial u_z}{\partial x}\frac{p_z p_x}{p}\frac{dn_\tau^0}{dp}. \tag{24}$$

As $F = -\eta\frac{\partial u_z}{\partial x}$, the shear viscosity can be calculated

from Eqs. (7) and (24) as

$$\eta = \sum_\tau -\frac{d}{(2\pi)^3} \int \tau_\tau(p) \frac{p_z(p_z - mu_z)p_x^2}{pm_\tau^\star} \frac{dn_\tau^0}{dp} dp_x dp_y dp_z$$

$$= \sum_\tau -\frac{d}{(2\pi)^3} \int \tau_\tau(p) \frac{p_z^2 p_x^2}{pm_\tau^\star} \frac{dn_\tau^\star}{dp} dp_x dp_y dp_z \qquad (25)$$

where $p = \sqrt{p_x^2 + p_y^2 + p_z^2}$ and $n_\tau^\star$ is the local momentum distribution. The second equality sign comes from that the shear viscosity is independent of the magnitude of the flow and $u_z = 0$ is chosen.

IV. RESULTS AND DISCUSSIONS

The momentum dependence of the total relaxation time for a nucleon and that for the nucleon to collide with other ones of same or different isospin in symmetric and neutron-rich nuclear matter are displayed in Fig. 3. A smaller relaxation time means the nucleon on average experiences more frequent collisions. A constant cross section would make the relaxation time decrease with increasing momentum, as higher-momentum nucleons are more likely to collide with others. Using the energy-dependent free-space nucleon-nucleon cross sections, there are peaks around $p = 500$ MeV, corresponding to the minimum values of the free cross sections as shown in Fig. 2. Due to the smaller effective masses of nucleons in the nuclear medium, which leads to smaller in-medium nucleon-nucleon cross sections, the relaxation times are larger. In symmetric nuclear matter, τ_τ, τ_τ^{same} and τ_τ^{diff} are the same for nucleons of different isospins. In neutron-rich nuclear matter, τ_n^{same} are smaller while τ_p^{same} are larger compared with that in symmetric nuclear matter, due to larger chances for nn collisions while smaller chances for pp collisions. In addition, τ_n^{diff} becomes larger while τ_p^{diff} becomes smaller, due to a smaller number of protons and a larger number of neutrons to collide with, respectively. It is seen that there are always more chances for collisions between nucleons with different isospins than those with same isospin, mainly because of the larger degeneracy factor for τ^{diff} than τ^{same} as in Eqs. (15) and (16) and the larger cross section of $\sigma_{\tau,-\tau}$ over $\sigma_{\tau,\tau}$. The total relaxation time is dominated by the smaller one, i.e., τ^{diff}. Thus $\tau_n > \tau_p$ is found in neutron-rich nuclear matter, and they are both of the magnitude only a few fm/c at $\rho = \rho_0$ and $T = 50$ MeV.

In Fig. 4 the effects of density and temperature on the relaxation time are displayed. It is seen that compared with the case at $T = 50$ MeV, the relaxation time is generally larger at $T = 10$ MeV, due to the fact that the nucleons are less energetic at lower temperatures. Furthermore, there appears a peak around $p = 270$ MeV indicating a stronger Pauli blocking effect near the Fermi surface. This can be understood as nucleons near the Fermi surface are more likely to collide with those below the
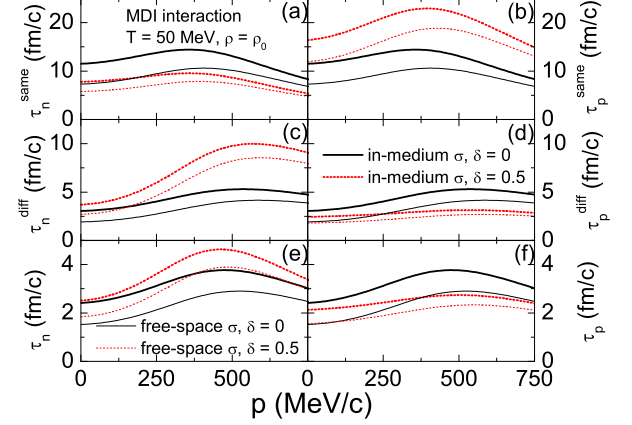

FIG. 3: (color online) Momentum dependence of the total relaxation time and the relaxation time for the nucleon to collide with other ones of same or different isospin in symmetric ($\delta = 0$) and neutron-rich ($\delta = 0.5$) nuclear matter.

Fermi surface due to larger cross sections at lower center-of-mass energy, but these collisions are largely blocked at $T = 10$ MeV. At $\rho = 2\rho_0$ the peaks move to a higher momentum and are even stronger, as the Fermi momentum is higher and the Pauli blocking effect is stronger due to the less diffusive distribution function as shown in Fig. 1. Again the relaxation times are larger from smaller in-medium cross sections, and at higher densities and lower temperatures this effect is larger due to smaller nucleon effective masses.
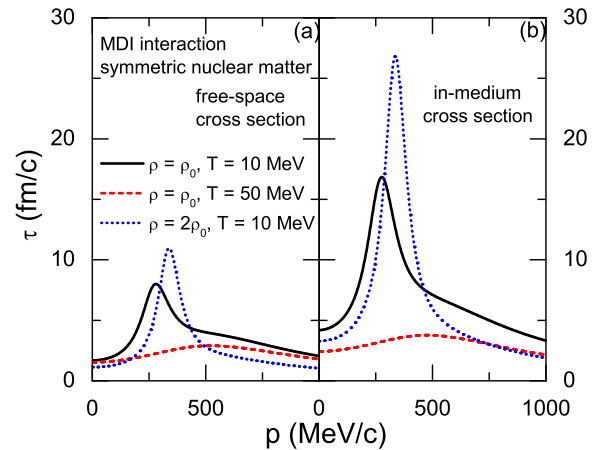

FIG. 4: (color online) Momentum dependence of the total relaxation time at different densities and temperatures in symmetric nuclear matter from free-space cross sections (left panel) and in-medium cross sections (right panel).

The specific viscosity, i.e, the ratio of the shear viscosity over the entropy density, is shown in upper panels of Fig. 5 as a function of the temperature for different densities (panel (a)) and as a function of the density for different temperatures (panel (b)) in symmetric and neutron-rich nuclear matter from free-space nucleon-nucleon cross sections. The lower bound $\eta/s \sim \hbar/4\pi$ obtained by the Anti de Sitter/conformal field theory (AdS/CFT) correspondence [35] is also shown by dotted lines for reference. The specific viscosity decreases with increasing temperature, as a result of more frequent collisions and weaker Pauli blocking effect at higher temperatures. Although the effective mass decreases with increasing density, which leads to a larger flux between flow layers as in Eq. (7), and a larger relative velocity between nucleons in Eqs. (15) and (16), the Pauli blocking effect is stronger at higher densities. The combined effects lead to an increasing trend of the specific viscosity with increasing density at lower temperatures, but a slightly decreasing trend with increasing density at higher temperatures when the Pauli blocking effect is much weaker. Furthermore, it is interesting to seen that the specific viscosity is larger in neutron-rich nuclear matter than in symmetric nuclear matter at all the densities and temperatures, especially at lower temperatures. This is because that the neutron relaxation time is larger than proton in neutron-rich nuclear matter and it contributes more to the total shear viscosity according to Eq. (25) due to a less diffusive neutron momentum distribution function. At lower temperatures, this effect is larger because of the larger difference between $\sigma_{\tau,\tau}$ and $\sigma_{\tau,-\tau}$, stronger Pauli blocking effect on neutrons, and less diffusive momentum distribution of neutrons as in Eq. (25).

The density and temperature dependence of the specific viscosity from in-medium cross sections are shown in the lower panels of Fig. 5. Compared with the results from free-space nucleon-nucleon cross sections, the specific viscosity is much larger at lower temperatures and higher densities, when the in-medium cross sections are smaller from smaller in-medium effective masses. The isospin effect on the specific viscosity is somehow smaller, compared with the results from free-space nucleon-nucleon cross sections, due to the isospin-dependent modification on the in-medium cross sections. As the effective mass of neutrons is larger than that of protons in neutron-rich nuclear matter, the isospin effect on τ_n is smaller from in-medium cross sections than that from free-space cross sections, as shown in panel (e) of Fig. 3. At $T = 50$ MeV, the specific viscosity is only about $4 \sim 5 \frac{\hbar}{4\pi}$, which is already close to the value of QGP extracted from the transverse momentum spectrum and elliptic flow using the viscous hydrodynamic model [36]. The specific viscosity obtained in this way is similar to that extracted from the BUU model calculation using the Green-Kubo formulas [22], which is around $20 \sim 30 \frac{\hbar}{4\pi}$ at lower energies and reduces to as low as $6 \frac{\hbar}{4\pi}$ at higher energies. The density and temperature dependence of the specific viscosity at lower temperatures are
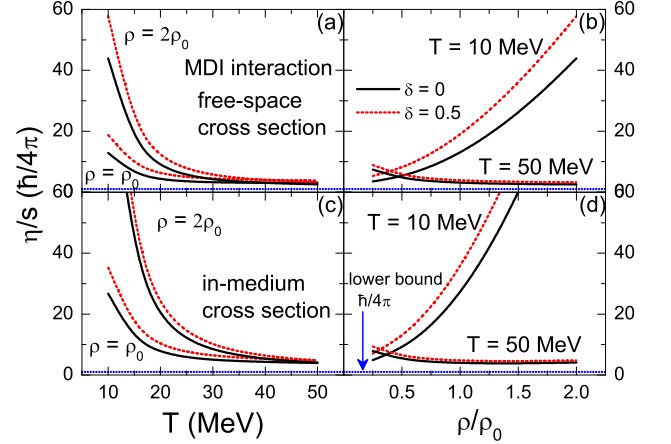

FIG. 5: (color online) Specific viscosity as a function of the temperature at $\rho = \rho_0$ and $\rho = 2\rho_0$ (left panels) and that as a function of the density at $T = 10$ MeV and $T = 50$ MeV (right panels) for symmetric ($\delta = 0$) and neutron-rich ($\delta = 0.5$) nuclear matter from free-space cross sections (upper panels) and in-medium cross sections (lower panels). The lower bound of the specific viscosity is also shown by dotted lines for reference.
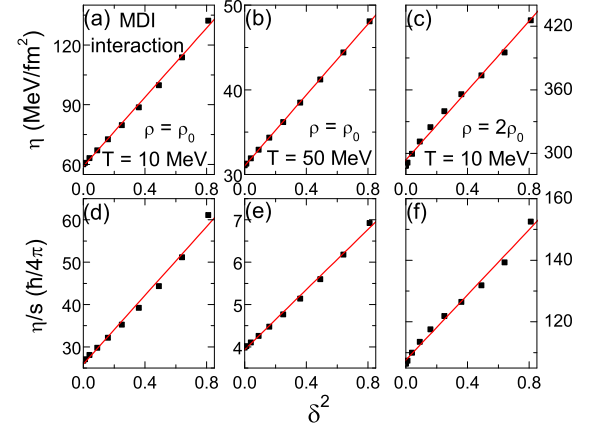
also similar to those in Refs. [18, 19],

FIG. 6: (color online) Shear viscosity η and specific viscosity η/s as functions of isospin asymmetry δ^2 for different densities and temperatures. The solid lines are from the linear fit.

It will be interesting to study in detail how the shear viscosity η and the specific viscosity η/s change with the isospin asymmetry δ, which is shown in Fig. 6. It is seen that both η and η/s roughly satisfy the parabolic

approximation

$$\eta(\rho, T, \delta) \approx \eta(\rho, T, \delta = 0) + \eta_{sym}(\rho, T)\delta^2, \qquad (26)$$

$$\left(\frac{\eta}{s}\right)(\rho, T, \delta) \approx \left(\frac{\eta}{s}\right)(\rho, T, \delta = 0) + \left(\frac{\eta}{s}\right)_{sym}(\rho, T)\delta^2, \qquad (27)$$

where the coefficients $\eta_{sym}(\rho, T)$ and $\left(\frac{\eta}{s}\right)_{sym}(\rho, T)$ are comparable to $\eta(\rho, T, \delta = 0)$ and $\left(\frac{\eta}{s}\right)(\rho, T, \delta = 0)$, respectively. The large isospin effect is also observed in results from the Brueckner theory [23]. The parabolic approximation is good even for very large isospin asymmetry, and it seems to be better at lower densities or higher temperatures.

V. CONCLUSIONS

In this paper I discussed the specific viscosity from the relaxation time approach by using the MDI interaction and the nucleon-nucleon cross sections from the experimental data modified by the in-medium effective masses as used in the IBUU transport model calculations. In neutron-rich nuclear matter, the relaxation time of neutrons increases while that of protons decreases, compared with that in symmetric nuclear matter. The specific viscosity decreases with increasing temperature because of more frequent collisions and weaker Pauli blocking effect. At lower temperatures, the specific viscosity increases with increasing density due to increasing effect of Pauli blocking while at higher temperatures it slightly decreases with increasing density due the smaller in-medium effective masses. The specific viscosity increases with increasing isospin asymmetry, mainly from the larger relaxation time of neutrons in neutron-rich nuclear matter. Both the shear viscosity and specific viscosity roughly follow the parabolic approximation with respect to the isospin asymmetry.

As in this frame work, the effect of the interaction on the specific viscosity only comes from the effective mass, i.e., the momentum dependence of the single-particle potential, the value of x, which determines the density dependence of the symmetry energy, will not affect the results. In reality, the transitive matrix $T_{\tau, \tau'}$ will also be modified in the medium, especially at higher densities. In a more realistic Brueckner-Hartree-Fock calculation [37], the in-medium cross section is calculated by consistently taking account of the two-body and three-body nucleon forces. It was found that the in-medium cross section is more isotropic compared with the cross section in free space as the forward and backward peaks are largely reduced, and including the three-body force would further reduce the nucleon-nucleon cross section. An isotropic cross section generally leads to a smaller viscosity than an anisotropic one with forward and backward peaks as the effective transport cross section is larger in the former case, while including the contribution from the three-body force seems to increase the viscosity. In addition, the system is assumed to consist of uniform nuclear matter in the present study. At higher densities and/or temperatures, inelastic nucleon-nucleon collisions such as $NN \to N\Delta$ become important, and Δ resonances and pions will be abundantly produced. At lower densities and/or temperatures, liquid-gas phase transition will occur and clusters will be formed. All these will affect the viscosity of the system.

[1] G.F. Bertsch and S. Das Gupta, Phys. Rep. **160**, 189 (1988).
[2] C. Gale, G. Bertsch, and S. Das Gupta, Phys. Rev. C **35**, 1666 (1987).
[3] D.H. Youngblood, H.L. Clark, and Y.W. Lui, Phys. Rev. Lett. **82**, 691 (1999).
[4] L.W. Chen, C.M. Ko, and B.A. Li, Phys. Rev. Lett. **94**, 032701 (2005).
[5] G.C. Yong, B.A. Li, and L.W. Chen, Phys. Rev. C **74**, 064617 (2006).
[6] G.C. Yong, B.A. Li, L.W. Chen, and X.C. Zhang, Phys. Rev. C **80**, 044608 (2009).
[7] Z.G. Xiao, B.A. Li, L.W. Chen, G.C. Yong, and M. Zhang, Phys. Rev. Lett. **102**, 062502 (2009).
[8] B.A. Li, L.W. Chen, and C. M. Ko, Phys. Rep. **464**, 113 (2008).
[9] W. Schmidt, U. Katscher, B. Waldhauser, J.A. Maruhn, H. Stöcker, and W. Greiner, Phys. Rev. C **47**, 2782 (1993).
[10] A. Peshier and W. Cassing, Phys. Rev. Lett. **94**, 172301 (2005).
[11] A. Majumder, B. Müller, and X.N. Wang, Phys. Rev. Lett. **99**, 192301 (2007).
[12] Z. Xu and C. Greiner, Phys. Rev. Lett. **100**, 172301 (2008).
[13] J.W. Chen, H. Dong, K. Ohnishi, and Q. Wang, Phys. Lett. **B685**, 277 (2010).
[14] A. Muronga, Phys. Rev. C **69**, 044901 (2004).
[15] J.W. Chen and E. Nakano, Phys. Lett. **B647**, 371 (2007).
[16] N. Demir and S.A. Bass, Phys. Rev. Lett. **102**, 172302 (2009).
[17] S. Pal, Phys. Lett. **B684**, 211 (2010).
[18] P. Danielewicz, Phys. Lett. **B146**, 168 (1984).
[19] L. Shi and P. Danielewicz, Phys. Rev. C **68**, 064604 (2003).
[20] J.W. Chen, Y.H. Li, Y.F. Liu, and E. Nakano, Phys. Rev. D **76**, 114011 (2007).
[21] S. Pal, Phys. Rev. C **81**, 051601(R) (2010).
[22] S.X. Li, D.Q. Fang, Y.G. Ma, and C.L. Zhou, Phys. Rev. C **84**, 024607 (2011).

[23] H.F. Zhang, U. Lombardo, and W. Zuo, Phys. Rev. C **82**, 015805 (2010).

[24] S. Jeon, Phys. Rev. D **52**, 3591 (1995).

[25] R. Kubo, Rep. Prog. Phys. **29**, 255 (1966).

[26] K. Huang, *Statistical Mechanics*, 2nd edition (John Wiley & Sons, New York, 1987).

[27] M.M. Abu-Samreh and H.S. Köhler, Nucl. Phys. **A552**, 101 (1993).

[28] C.B. Das, S. Das Gupta, C. Gale, and B.A. Li, Phys. Rev. C **67**, 034611 (2003).

[29] J. Xu and C.M. Ko, Phys. Rev. C **82**, 044311 (2010).

[30] J. Xu, L.W. Chen, B.A. Li, and H.R. Ma, Phys. Rev. C **75**, 014607 (2007).

[31] B.A. Li and L.W. Chen, Phys. Rev. C **72**, 064611 (2005).

[32] B.A. Li, Phys. Rev. C **69**, 064602 (2004).

[33] S.K. Charagi and S.K. Gupta, Phys. Rev. C **41**, 1610 (1990).

[34] V.R. Pandharipande and S.C. Pieper, Phys. Rev. C **45**, 791 (1992).

[35] P.K. Kovtun, D.T. Son, and A.O. Starinets, Phys. Rev. Lett. **94**, 111601 (2005).

[36] H.C. Song, S.A. Bass, U. Heinz, T. Hirano, and C. Shen, Phys. Rev. Lett. **106**, 192301 (2011).

[37] H.F. Zhang, Z.H. Li, U. Lombardo, P.Y. Luo, F. Sammarruca, and W. Zuo, Phys. Rev. C **76**, 054001 (2007), and references therein.